Radiochim. Acta **90**, 315–321 (2002)

X-ray absorption fine structure spectroscopy of plutonium complexes with *bacillus sphaericus*

By P. J. Panak[1], C. H. Booth[1], D. L. Caulder[1], J. J. Bucher[1], D. K. Shuh[1] and H. Nitsche[1,2,*]

[1] Lawrence Berkeley National Laboratory (LBNL), Chemical Sciences Division, The Glenn T. Seaborg Center, Berkeley, CA 94720, USA
[2] University of California at Berkeley, Department of Chemistry, Berkeley, CA 94720, USA

(Received September 12, 2001; accepted in revised form January 14, 2002)

XANES / EXAFS / Plutonium(VI) / Biosorption / Soil bacteria / Bacillus sphaericus

Summary. Knowledge of the plutonium complexes formed with bacterial cells is critical for predicting the influence of microbial interactions on the migration behavior of actinides in the environment. This investigation describes the interaction of plutonium(VI) with cells of the aerobic soil bacteria, *Bacillus sphaericus*. The studies include the quantification of carboxylate and phosphate functional groups on the cell walls by potentiometric titration and the determination of the plutonium speciation by X-ray absorption fine structure (XAFS). Extended-XAFS (EXAFS) was used to determine the identity of the Pu(VI) interfacial complex with the bacteria, and the Pu(VI) was found primarily bound to phosphate groups on the cell surface. No carboxylate complexation was detected.

Introduction

Microbial processes can have an important influence on the migration behavior of actinides in natural systems. Microorganisms can oxidize or reduce multivalent actinides, cause precipitation of radionuclides and biodegradation of solvents and complexants coexisting in the soil or in waste streams, and form strong complexes with the actinide contaminants [1]. These processes can cause either mobilization or immobilization of the radionuclides. *Bacilli* are ubiquitous in nature and because of their ability to form spores they survive even under very harsh conditions [2]. Earlier investigations with different strains of *Bacillus* have shown that *Bacilli* form strong surface complexes with uranium(VI) [3]. The characterization of the U(VI)-*Bacilli* complexes with time-resolved laser fluorescence spectroscopy and X-ray absorption fine structure spectroscopy (XAFS) have proven that uranium(VI) is bound to phosphate groups [3, 4]. Contrary to U(VI), plutonium species are redox active and can coexist in several oxidation states, *i.e.*, 4+, 5+, and 6+, in aqueous solution under environmental conditions [5]. In particular, hexavalent plutonium has a high solubility and is quite stable under aerobic conditions, and, therefore, has the potential of being transported from contaminated areas to environments accessible by humans. Sorption studies with Pu(VI) have shown that the interaction with the biomass causes changes of the oxidation state [6]. Knowledge of the plutonium complexes formed with bacterial cells is very important for predicting the influence of microbial interactions on the migration behavior of actinides in the environment. XAFS spectroscopy is a useful tool for characterizing the speciation of metal ions in a variety of complex experimental systems. XAFS is composed of two component spectroscopies, X-ray absorption near edge structure (XANES) and extended X-ray absorption fine structure (EXAFS), which provide element specific oxidation state and local structure information, respectively.

Our research focuses on the interaction of plutonium(VI) with cells of *Bacillus sphaericus*. The number of functional groups on the cell surface are quantified by potentiometric titration and compared to chemical analysis results of isolated cell walls. The studies include determination of the different plutonium oxidation states after varying contact times with the biomass by XANES, and characterization of the Pu(VI) complex with *Bacillus sphaericus* cells by EXAFS.

Experimental

Potentiometric proton titration

The bacterial strain (*Bacillus sphaericus* ATCC 14577) was grown under aerobic condition in 500 mL nutrient medium (8 g/L nutrient broth, Difco) at 22 °C. The biomass was harvested by centrifugation (6000 × g). The cells were washed four times each with 50 mL physiological NaCl-solution (0.9%).

The potentiometric titration to determine the amount of phosphorus on the cell walls was performed in 0.01 M $NaClO_4$ at 23 °C under nitrogen using an ORION 960 Autochemistry System. The system consists of an ORION 960 module, an EA 940 pH/ISA meter, an autodispenser, and an electrode tower. The biomass (5.07 $mg_{dry\ weight}$) was suspended in 20 mL 0.01 M $NaClO_4$ and titrated with 0.01 M NaOH (CO_2 free). Blank titrations were carried out under the same conditions. The binding and removal of protons from the cell walls at a given pH was determined by subtracting the amount of titrant added to the blank solution from those of the cell wall titration. Titrant was added when

*Author for correspondence (E-mail: Hnitsche@lbl.gov).

dmV/d*t* was less than 0.5 mV per 1 min. The change of pH was approximately 1 unit in 20 minutes. Additionally, titrations using 0.01 M HCl and 0.01 M NaOH were performed to investigate possible hysteresis of the acid and base titration curves.

Biosorption

The ^{239}Pu was purified by ion exchange chromatography (Dowex AG1-X8 anion resin), the eluate was evaporated twice with conc. HNO_3 to near dryness, and the plutonium was oxidized to Pu(VI) with concentrated $HClO_4$. For our biosorption studies, we contacted different amounts of biomass with 30.4 mg/L Pu(VI) in 1.5 mL 0.9% NaCl-solution at pH 4.4 for six hours. The biomass was varied from 0.07 $g_{dry\ weight}$/L to 1.17 $g_{dry\ weight}$/L. Plutonium concentrations were measured by liquid scintillation counting using a LKB Wallac, 1219 Rackbeta liquid scintillation counter.

XAFS

Two hundred and fifty micro liters of the ^{239}Pu(VI) stock solution (5.7×10^{-3} mol/L, 0.1 M $HClO_4$) were used for XAFS measurements to obtain the Pu(VI) reference spectrum. Pu(V) was prepared by electrochemical reduction of Pu(VI). The reduction was carried out at pH 3 and $+0.450$ volts (*vs*. Ag/AgCl). Details on the preparation of different oxidation states and the equipment used are described elsewhere [7, 8]. The final solution (2.4×10^{-3} mol/L, pH 3, 0.1 M $NaClO_4$) contained more than 99% Pu(V). Oxidation state purity was verified by optical absorption spectroscopy. $PuO_2(H_2PO_4)_2$ was precipitated at pH 3.5 by adding a 0.1 M NaH_2PO_4 solution to the Pu(VI) solution (pH 3.5). After removing more than 90% of the water, the sample was measured as wet paste. The bacterial samples for XANES were prepared by incubating 1350 μL of the bacterial stock solution (8.34 $g_{dry\ weight}$/L) in physiological NaCl solution with 0.84 mg Pu(VI) at pH 4.4 and were measured as wet pastes.

For the preparation of the pure Pu(VI) *Bacillus*-complex used for EXAFS measurement, we removed the Pu(VI) which remained in solution and the Pu(V) which was formed by bacteria-mediated reduction of Pu(VI) by washing the biomass with 1 mL physiological NaCl solution before the sample was transported to the beamline. The sample (wet paste) was measured within six hours after the last washing process. All samples were placed in 250 μL plastic tubes prior to the XAS measurement.

Plutonium XAFS spectra were collected at the Stanford Synchrotron Radiation Laboratory on wiggler beam line 4-1 using a half-tuned Si (220) double-crystal monochromator. Measurements were performed in fluorescence mode using a 4-element Ge fluorescence detector [9] at the Pu L_{III} edge. Energy calibration was performed by simultaneously measuring the XANES of a PuO_2 reference. Three scans were collected on each sample and averaged to improve the statistics. All data reduction and fits utilized standard procedures [10, 11]. In particular, data from the Ge detector data were corrected for dead time. Curve-fitting amplitudes and phases were calculated using FEFF7.

Solvent extraction

To verify the distribution of oxidation states obtained from the XANES, the Pu oxidation state was also determined by solvent extraction methods. Five hundred μL of the solution were extracted with 500 μL of 0.5 M thenoyltrifluoroacetone (TTA) in xylene and 500 μL di(2-ethylhexyl)phosphoric acid (HDEHP) in toluene, respectively. The extractions were performed according to Ref. [12]. The Pu concentrations of all phases were measured by liquid scintillation counting.

Results

Determination of the phosphate groups on the cell surface

The cell walls of bacteria are porous three-dimensional macromolecular networks. The main cell wall polymer of Gram-positive bacteria is peptidoglycan. Besides the peptidoglycan other macromolecules like teichoic acid, (lipo)polysaccharides, (lipo)proteins, and enzymes may be present. These macromolecules carry carboxylic, phosphate and amino groups. Bacterial cell walls have amphoteric character. They also possess more anionic than cationic groups, and most bacterial cells have an isoelectric point below pH 4 [13, 14].

The results of the proton titration of *Bacillus sphaericus* are given in Fig. 1. Under these experimental conditions, we observed no hysteresis in the acid and base titration curves. This indicates that the charging process can be considered as reversible which implies the charged groups within the cell wall are in equilibrium with the surrounding electrolyte. The point of zero charge (PZC) was at pH 4.1, which is in good agreement with literature values [14] for other Gram-positive bacteria.

The inflection points of the titration curve show distinct pH regions for different classes of functional groups. We used the reciprocal differential titration curve approach (also shown in Fig. 1) to determine these pH regions better. The maxima of the differential titration curve indicate the equivalence points of the classes of functional groups. The pK values determined are the average value for one class of functional groups. The pK values of a particular functional

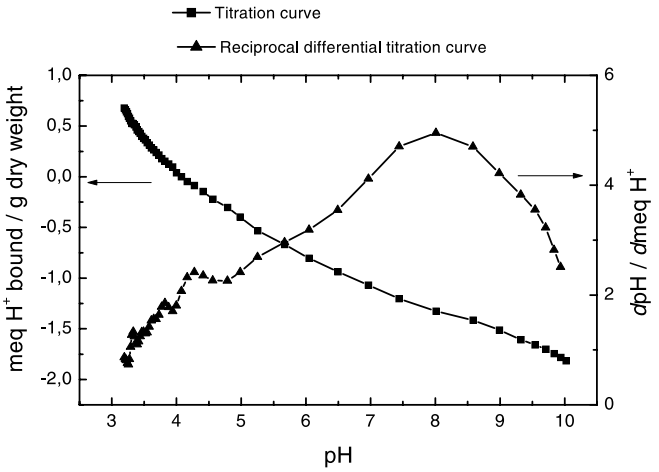

Fig. 1. Titration curve of *Bacillus sphaericus* (left scale) and the reciprocal differential titration curve (right scale) as a function of pH.

group may be higher or lower, depending on neighboring groups and their binding to the cell wall. The small maximum at pH 4.3 can be attributed to carboxylic groups on the cell surface. This value is in very good agreement with literature values for carboxylic groups of different Gram-positive bacteria which were found to be between pH 4.1 and 4.7 [14]. The main maximum at pH 8.3 was identified as the equivalent point of the dissociation of the second hydrogen ion of the phosphate group and is also in good agreement with literature data [14]. Generally, the dissociation constants of functional groups of polyelectrolytes differ from that of isolated groups ($pK(H_2PO_4^-/HPO_4^{2-}) = 7.2$). This difference is due to the influence of the organic molecule to which the functional groups are bound, and also to the electrostatic interactions with neighboring groups. This so-called polyelectrolyte effect increases with decreasing ionic strength. The pK for the amino groups is between 11 and 12 [14] and the one for the dissociation of the first hydrogen ion of the phosphate groups is below 2.25 [14], and are beyond the pH region of our titration.

The number of phosphate groups was determined from the differential titration curves as a function of the amount of protons bound to the cell wall (not shown). The analysis of the titration data yielded a value of $0.89 \pm 0.09\,\mathrm{mmol/g_{dry\ weight}}$ for the *Bacillus sphaericus* strain studied. This number compares well with those obtained by chemical analysis of isolated cell walls of different *Bacillus* strains ($0.5–1.6\,\mathrm{mmol/g_{dry\ weight}}$) [4].

Sorption studies provide information on the amount of Pu bound to different amounts of biomass (see Fig. 2). The results show that not all phosphate groups on the cell surface determined by acid/base titration are available for binding of Pu(VI). We calculated a maximum loading with Pu(VI) on the biomass of 39% (compared to the total number of available phosphate groups) for the low biomass concentrations. With increasing biomass concentration, the cells agglomerate [6] and the number of available phosphate groups decreases relatively to the dry weight. As shown in Fig. 2 (right scale), this leads to a non-linear decrease of the $[Pu]_{bound}$/[phosphate] fraction with increasing bacterial concentrations. The molar ratios of P to Pu_{bound} are in excellent agreement with our earlier results on U(VI) with different *Bacillus* strains [4]. The molar ratios of P to U_{bound} were found to be between 3 : 1 and 10 : 1 which reveals that only specific phosphate groups of the cell walls are involved in the complexing of U(VI).

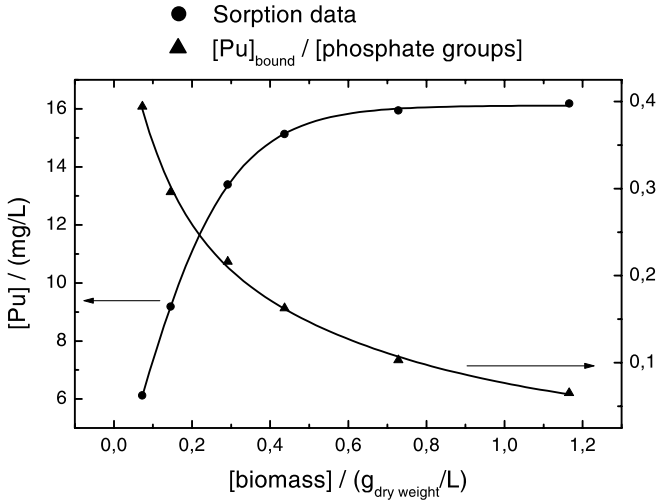

Fig. 2. Sorption of Pu(VI) ($[Pu]_{initial} = 30.4\,\mathrm{mg/L}$) (left scale) and changes of the molar ratio of Pu_{bound} to the phosphate groups on the cell surface (right scale) with increasing biomass concentration.

XAFS of plutonium complexes with *Bacillus sphaericus*

Determination of Pu oxidation states by XANES

Based on our earlier results on microbial interaction of Pu(VI) with bacteria, we developed a model to describe the interaction of Pu(VI) with aerobic soil bacteria [6]. The overall mechanism includes three processes with different time scales. In a first step, Pu(VI) is bound to phosphate groups of the biomass. This process is characterized by fast kinetics and depends strongly on the amount of biomass that determines the number of available binding sites on the cells. In a second step, a part of the cell-bound Pu(VI) is reduced to Pu(V) by interaction with the biomass. This process is much slower compared to the binding of Pu(VI) to the biomass. After 24 hours, one third of the initial Pu(VI) was reduced to Pu(V). Due to the weak complexation ability of the PuO_2^+, the Pu(V) formed was found in solution. At that time, no Pu(IV) could be detected. Long-term studies have shown that after a contact time of one month, 16.1% Pu(IV) was formed resulting from disproportionation of Pu(V) and autoreduction of Pu(VI) (third process). The amount of Pu(IV) formed is strongly dependent on the initial Pu(VI) concentration. The plutonium concentration used for XAFS was 30 times higher than that of our mechanistic studies in [6]. Therefore, we expected to find a higher amount of Pu(IV) in these samples.

Plutonium oxidation states are often determined by measuring the main L_{III} absorption energy (generally taken as the first inflection point of the edge) relative to a known standard [15–17]. In addition to the energy shifts of the Pu(IV), Pu(V) and Pu(VI) standards relative to the PuO_2 reference (1.9 ± 0.1 eV, 0.2 ± 0.1 eV, and 2.3 ± 0.1 eV, respectively), there is a feature on the high energy side of the white line in the Pu(V) and Pu(VI) standard spectra due to the $Pu-O_{ax}$ multiple scattering (see discussion regarding EXAFS below)

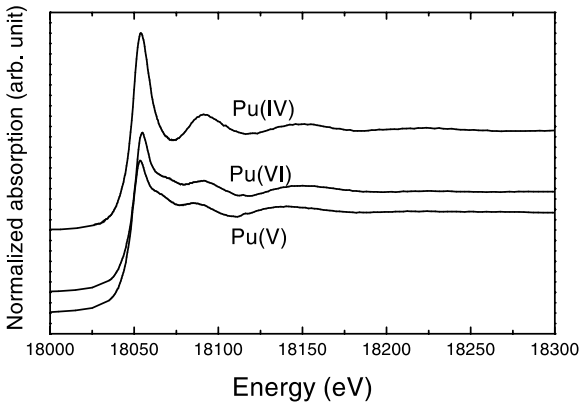

Fig. 3. X-ray absorption spectra of Pu(IV), Pu(V) and Pu(VI). Note the feature near 18 070 eV in the Pu(V) and Pu(VI) spectra that is due to $Pu-O_{ax}$ multiple scattering.

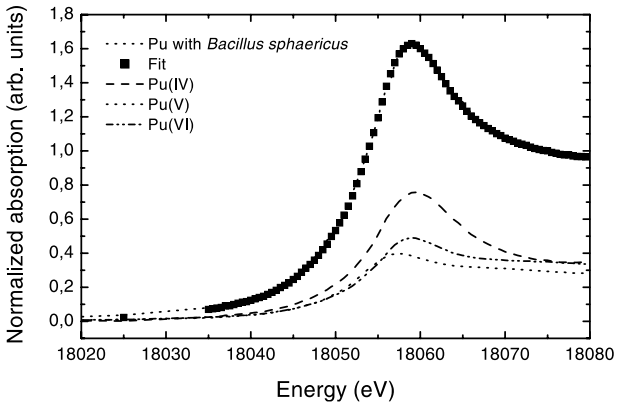

Fig. 4. Determination of oxidation states of Pu by fitting the XANES spectrum after 9 days of contact with *Bacillus sphaericus* to the weighted sum of standard spectra between 18 000 and 18 080 eV.

(Fig. 3). These energy and shape differences allow for a determination of the relative concentrations of the Pu species by fitting the bacteria spectra to the weighted sum of the appropriate standard spectra between 18 000 and 18 080 eV. This procedure generally gives an accurate measurement of the relative Pu(IV) concentration; however, the small edge shift and shape difference between the Pu(V) and Pu(VI) standard spectra causes correlations between their concentration measurements. To minimize these correlations, we fix the standard edge energies in the fits, allowing only the amplitudes to vary. Moreover, we compare the results from these XANES measurements to those obtained by solvent extraction with TTA and HDEHP. Solvent extraction allows a selective separation of different oxidation states of Pu even at low concentration levels between 10^{-6} and 10^{-10} mol/L.

Fig. 4 shows the plutonium near-edge spectrum (initially Pu(VI), [Pu] = 6.8 g/L) after 9 days of contact with *Bacillus sphaericus*. Analysis of the XANES spectrum (Table 1) shows that $32 \pm 10\%$ was still Pu(VI), whereas $28 \pm 12\%$ and $40 \pm 6\%$ were reduced to Pu(V) and Pu(IV), respectively. These results agree with the results from solvent extraction within estimated errors (Table 1).

EXAFS studies of the Pu(VI) complex with *Bacillus sphaericus*

In addition to the information on the valence of the central atom obtained from the near-edge structure, EXAFS measurements provide information on the local environment around the central atom such as the atomic number and the number of the neighboring atoms (N) and their distance from the central atom (R). For EXAFS spectroscopy of the Pu(VI) complex with *Bacillus sphaericus*, formed during the initial microbial interactions of Pu(VI) with aerobic soil bacteria, we prepared a sample with a very low content of Pu(IV) and Pu(V) (see experimental section). Both solvent extraction and XANES show that at the time the sample was measured (six hours after the last washing process) no Pu(IV) was formed and the content of Pu(V) was lower than 7.5%.

To better interpret the data of the Pu(VI)-*Bacillus* complex, we measured the EXAFS spectra of the Pu(VI) and the Pu(V) aquo ions in solution and the Pu(VI) phosphate precipitate $PuO_2(H_2PO_4)_2$. The Pu L_{III}-edge k^3-weighted EXAFS spectra, the corresponding Fourier transforms of the reference samples, and the theoretical fits are shown in Figs. 5 and 6. The results of the data analysis are summarized in Table 2. The Pu(V) and Pu(VI) dioxo-cations in the standard solutions are characterized by two doubly-bound axial oxygens at a short distance and their equatorial oxygens at a longer distance. As shown in Table 2, the axial and equatorial distances are 1.82 Å and 2.48 Å for the Pu(V)

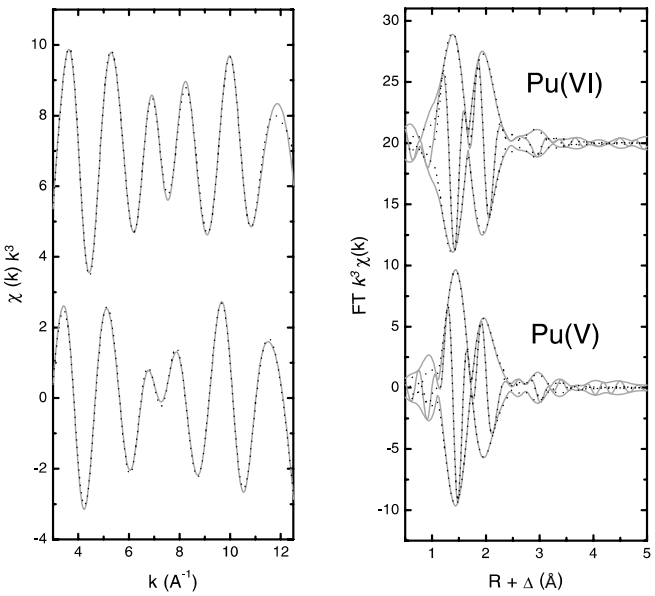

Fig. 5. Pu L_{III}-edge k^3-weighted EXAFS spectra (left) and the corresponding Fourier transforms (right) of the Pu(V) and the Pu(VI) reference samples and the theoretical fits (dotted line). The outer envelope of the Fourier transforms is the amplitude and the oscillating inner line is the real part of the complex transform. The transform range in this and other figures is 2.5–13 $Å^{-1}$ and Gaussian narrowed with a 0.3 $Å^{-1}$ window. The fit range is 1.2–3.5 Å. The Fourier transforms are not corrected for EXAFS phase shifts, so that FT peak position of a given peak does not equal the pair distance *R*.

Table 1. Oxidation state distribution of plutonium after 9 days contact with *Bacillus sphaericus* determined by analysis of the XANES compared to oxidation states obtained by solvent extraction with 0.5 M TTA and 0.5 M HDEHP. Errors in the XANES measurements were determined from the covariance matrix and assuming that χ^2 divided by the degrees of freedom was equal to unity. Errors from solvent extraction are considered to be ~ 5%.

Experimental conditions	Oxidation state distribution by edge fitting of XANES spectra	Oxidation state distribution by solvent extraction
Bacillus sphaericus	40 (6)% Pu(IV)	40 (5)% Pu(IV)
[Pu] = 6.8 g/L	28 (12)% Pu(V)	36 (5)% Pu(V)
Contact time: 9 days	32 (10)% Pu(VI)	24 (5)% Pu(VI)

Table 2. EXAFS structural parameters of the Pu(V) and the Pu(VI) aquo ions, $PuO_2(H_2PO_4)_2$ and the Pu(VI)-*Bacillus sphaericus* complex in comparison to literature data (error in parentheses). Errors are the approximate absolute errors estimated by comparison to crystalline standards [10] or from a Monte Carlo technique whichever is larger [20]. Fits include the $Pu-O_{ax}$ multiple scattering peak and further peaks (usually oxygen) to phenomenologically account for overlap with the Pu−P peak, and as such their fit parameters are not shown.

Sample	Shell	R(Å)	N^a	σ(Å)
Pu(V)	$Pu-O_{ax}$	1.821 (5)	2	0.030 (3)
	$Pu-O_{eq}$	2.48 (1)	3.8 (4)	0.072 (7)
Pu(VI)	$Pu-O_{ax}$	1.759 (5)	2	0.047 (5)
	$Pu-O_{eq}$	2.42 (1)	4.7 (5)	0.067 (7)
$PuO_2(H_2PO_4)_2$	$Pu-O_{ax}$	1.787 (5)	2	0.049 (5)
	$Pu-O_{eq}$	2.37 (1)	4.3 (4)	0.10 (1)
	Pu−P	3.63 (3)	2.4 (3)	0.10 (1)
Pu(VI)-*Bacillus sphaericus* complex	$Pu-O_{ax}$	1.777 (5)	2	0.068 (7)
	$Pu-O_{eq}$	2.42 (1)	4.2 (4)	0.10 (1)
	Pu−P	3.71 (3)	1.5 (5)	0.072 (7)
Literature data				
Sample	Shell	R(Å)	N^a	σ(Å)
Pu(V)	$Pu-O_{ax}$	1.81	2	–
[16]	$Pu-O_{eq}$	2.47	4	–
Pu(VI)	$Pu-O_{ax}$	1.74	2	–
[16]	$Pu-O_{eq}$	2.40	6	–
Pu(VI)	$Pu-O_{ax}$	1.74	1.9	0.03
[17]	$Pu-O_{eq}$	2.42	4.4	0.07

a: N for $Pu-O_{ax}$ is fixed at 2 and $s_0^2 = 0.9$.

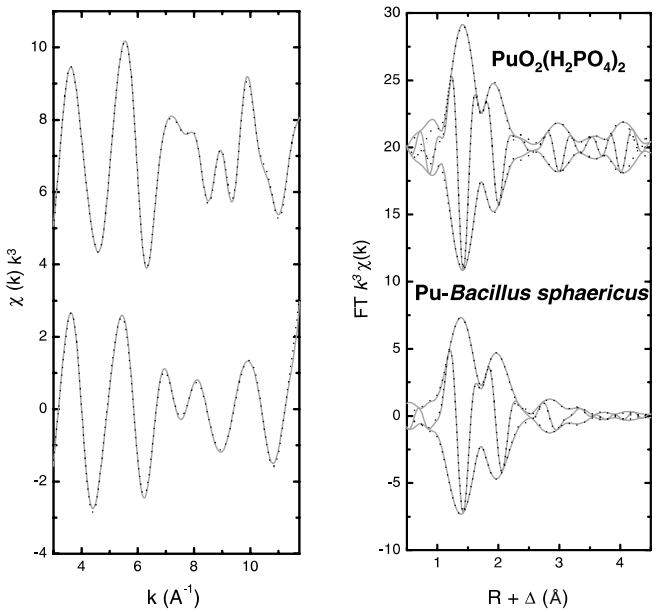

Fig. 6. Pu L_{III}-edge k^3-weighted EXAFS spectra (left) and the corresponding Fourier transforms (right) of $PuO_2(H_2PO_4)_2$ and the Pu(VI)-*Bacillus sphaericus* complex and the theoretical fits (dotted line). The fit range is 1.2–4.2 Å.

aquo ion and 1.76 Å and 2.42 Å for the Pu(VI) aquo ion, respectively. The Pu(VI) standard has a larger number of equatorial oxygens at a shorter distance compared to the Pu(V) standard. The increase of the oxidation state also causes a 0.06 Å contraction of the double bond. The structural parameters derived for the Pu(V) and Pu(VI) references are in very good agreement with literature data (also shown in Table 2) [16, 17].

As mentioned briefly in regards to the XANES, multiple scattering is known to occur for the collinear $Pu-O_{ax}$ pairs, giving a $Pu-O_{ms}$ peak in the EXAFS Fourier transform. This peak corresponds to an atom pair distance that is twice that of the $Pu-O_{ax}$ distance. This feature is visible in Fig. 3 just below 3 Å, corresponding to a $Pu-O_{ms}$ length of about 3.6 Å. We account for this peak in the fits to the EXAFS spectra by fixing the amplitude of the $Pu-O_{ms}$ peak to half of the amplitude of the $Pu-O_{ax}$ single scattering peak and the atom pair distance to twice that of the $Pu-O_{ax}$ distance. Fit parameters for this $Pu-O_{ms}$ peak are less reliable than single scattering peaks, especially for the Debye–Waller factor (σ). Generally speaking, all of the $Pu-O_{ms}$ σ measurements from fits reported in this work are smaller than physically reasonable considering thermal bond vibrations, and therefore the $Pu-O_{ms}$ contribution is overestimated.

Complexation of Pu(VI) with $H_2PO_4^-$ ligands in the $PuO_2(H_2PO_4)_2$ standard increases the bond length of the axial oxygens and decreases the equatorial oxygen distances. The distance between the plutonium and the axial oxygen atoms is 1.79 Å. The equatorial oxygen distance was found to be 2.37 Å which matches the average distance for monodentate coordination determined for uranyl systems [4]. The equatorial oxygen coordination number is 4.3 ± 0.3. Like the plutonyl standards, the spectrum of the plutonium phosphate precipitate exhibits a peak at about 3 Å, however it is stronger and has a different phase character than the spectra from the Pu(V) and Pu(VI) aquo ions. Although this peak has a $Pu-O_{ms}$ contribution as in the aquo ions, it is primarily caused by the scattering from the phosphorus atoms at a distance of 3.63 Å. The measured Pu−P coordination number is 2.4 ± 0.3. This measurement is consistent with the expected coordination of two from the composition of the precipitate.

The Pu(VI) atom of the Pu-*Bacillus* complex is also coordinated with 4 equatorial oxygen atoms, but the distance to the equatorial oxygens (2.42 Å) as well as the Pu-phosphorus distance (3.70 Å) are longer than in our Pu-phosphate model compound. The determination of the number of phosphorus

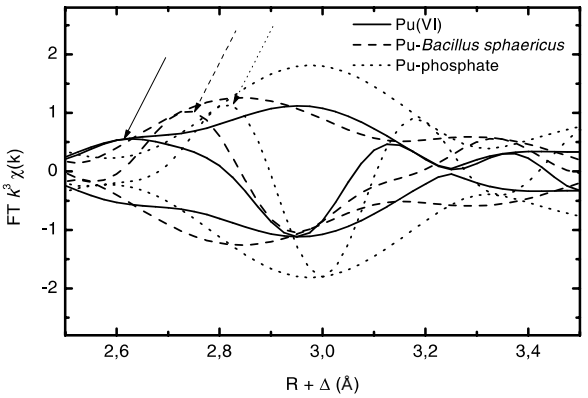

Fig. 7. Fourier transforms of the EXAFS spectra of the Pu(VI) reference solution, the Pu-*Bacillus* complex and the Pu-dihydrogen phosphate complex in the $R + \Delta$ (Å) region from 2.5 to 3.5 Å.

atoms is more complicated than in the model data because the Pu−P contribution is smaller and therefore interferes more strongly with the Pu−O_{ms} peak. To estimate the coordination number, we compare the spectrum of the Pu-*Bacillus* complex with those of the Pu(VI) aquo ion and the Pu-dihydrogen phosphate complex in the $R + \Delta$ (Å) region from 2.5 to 3.5 Å (Fig. 7). As shown in this figure, the maximum of the real part of the complex transform shifts from 2.62 Å for the Pu(VI) reference to 2.73 Å for the Pu-*Bacillus* complex and to 2.82 Å for the plutonium phosphate. In addition, the amplitude increases with increasing number of phosphorus atoms from 0 (Pu(VI) reference solution) to 2 ($PuO_2(H_2PO_4)_2$). Comparison with the reference spectra in the $R + \Delta$ region from 2.6 Å to 3.0 Å shows that the number of phosphorus atoms in the coordination sphere of the bacterial complex is probably lower than that of the Pu-phosphate. We determine an average coordination number both from these direct comparisons and from the fits of 1.5 ± 0.5 for the Pu(VI)-*Bacillus sphaericus* complex.

Discussion

Our results show that *Bacillus sphaericus* forms strong surface complexes with plutonium(VI). Similar to earlier investigations with U(VI), mainly phosphate groups on the cell surface are involved in Pu complexation. We obtain an average number of phosphate groups of 0.89 $mmol/g_{dry\ weight}$ for the strain used in our experiments but not all phosphate groups determined by acid/base titration are available for binding of the Pu. We calculate a maximum molar ratio of Pu_{bound} to P of 2.6 : 1.

Knowledge of the bacterial Pu(VI) complex is necessary for predicting the microbial impact on the migration behavior of Pu(VI) in the environment. We used EXAFS spectroscopy to determine the structural parameters of the Pu(VI) bacterial complex. Our results show that Pu(VI) is primarily bound to phosphate groups on the cell surface. No carboxylate complexation could be detected. This agrees with our earlier results on the complexation of U(VI) to different *Bacillus* strains [3, 4].

Related studies on the interaction of U(VI) with living cells, spores, heat-killed cells, and decomposed cells of *Bacillus sphaericus* by time-resolved laser fluorescence spectroscopy [18, 19] show that different phosphate complexes are formed. Using intact cells, the U(VI) is bound to organo-phosphate groups of the bacterial cells. With increasing age of the samples, the cells begin to lyse. During this process, inorganic phosphate is released and a uranyl phosphate precipitate is formed. The characterization of the released phosphate species by Raman spectroscopy [18] and the uranyl phosphate complexes by time-resolved laser-induced fluorescence spectroscopy (TRLFS) [18, 19] has shown that the bacteria release $H_2PO_4^-$ during decomposition which leads to the formation of $UO_2(H_2PO_4)_2$.

EXAFS spectroscopy of the Pu(VI) complex with *Bacillus sphaericus* confirms these results. The analysis of the EXAFS data not only provides information on the bond lengths and the coordination number of the axial and equatorial oxygens and the phosphorus atoms, it also shows that the Pu(VI) in our 6-hours sample is not precipitated as $PuO_2(H_2PO_4)_2$ by released phosphate. The feature of the k^3-weighted EXAFS spectra and the corresponding Fourier transforms of the bacterial complex differ significantly from those of the $PuO_2(H_2PO_4)_2$ precipitate. Furthermore, the bond lengths between the Pu(VI) and the equatorial oxygen as well as the phosphorus atoms are longer in the bacterial phosphate complex than in the Pu(VI) dihydrogen phosphate precipitate. The number of phosphorus atoms also decreases. In agreement with the results of U(VI), we conclude that Pu(VI) is bound to organo phosphate groups of the cell surface. Differentiation between complexes formed by interaction with bacteria is very important for studies in natural environmental systems where not only living metabolizing cells but also dead and even decomposed cells are present. Further studies on complexation of U(VI) with bacterially-related phosphate species as a function of age and status of the bacteria using EXAFS are under way.

In conclusion, we find that contrary to U(VI), which is stable under our experimental conditions [4, 18], Pu(VI) is reduced with increasing contact time to Pu(V) in the presence of aerobic soil bacteria [6]. Pu(IV) is also formed by disproportionation of Pu(V) and autoreduction of Pu(VI). We investigated the oxidation state distribution by fitting the XANES spectra by using Pu(IV), Pu(V) and Pu(VI) reference spectra. The results agree well with the oxidation state distribution obtained by solvent extraction. Near-edge spectroscopy allows easy detection of oxidation state changes even in very complex systems such as bacterial suspensions without disturbing the chemical equilibrium.

Acknowledgment. This work was supported in part by the Director, Office of Science, U.S. Department of Energy (DOE) under Contract No. DE-AC03-76SF00098 at LBNL. Part of this work was performed at SSRL which is also funded by the aforementioned DOE office.

References

1. Francis, A. J.: J. Alloys Compd. **271**–**273**, 78 (1998).
2. Slepecky, R., Hemphill, H.: The Genus *Bacillus*-Nonmedical. In: *The Prokaryotes*. Springer Verlag, Berlin (1991), pp. 1663–1696.
3. Panak, P. J., Raff, J., Selenska-Pobell, S., Geipel, G., Bernhard, G., Nitsche, H.: Radiochim. Acta **88**, 71 (2000).
4. Hennig, C., Panak, P. J., Reich, T., Rossberg, A., Raff, J., Selenska-Pobell, S., Matz, W., Bucher, J. J., Bernhard, G., Nitsche, H.: Radiochim. Acta **89**, 625 (2001).
5. Choppin, G. R.: Radiochim. Acta **43**, 82 (1988).

6. Panak, P. J., Nitsche, H.: Radiochim. Acta **89**, 499 (2001).
7. Cohen, D. J.: Inorg. Nucl. Chem. **18**, 207 (1961).
8. Nitsche, H., Edelstein, N.: Radiochim. Acta **39**, 23 (1985).
9. Bucher, J. J., Edelstein, N. M., Osborne, K. P., Shuh, D. K., Madden, N., Luke, P., Pehl, D., Cork, C., Malone, D., Allen, P. G.: Rev. Sci. Inst. **67**, 1 (1996).
10. Li, G. G., Bridges, F., Booth, C. H.: Phys. Rev. B **58**, 2995 (1995).
11. Hayes, T. M., Boyce, J. B.: In: *Solid State Physics*. (Ehrenreich, H., Seitz, F., Turnbull, D., eds.) Academic, New York (1982) Vol. 37, p. 173.
12. Nitsche, H., Lee, C., Gatti, R. C.: J. Radioanal. Nucl. Chem. **124**/**1**, 171 (1988).
13. Harden, V. P., Harris, J. O.: J. Bacteriol. **65**, 198 (1952).
14. van der Wal, A., Norde, W., Zehnder, A. J. B., Lyklema, J.: Colloids Surf. B: Biointerfaces **9**, 81 (1997).
15. Conradson, S. D., Al Mahamid, I., Clark, D. L., Hess, N. J., Hudson, E. A., Neu, M. P., Palmer, P. D., Runde, W. H., Tait, C. D.: Polyhedron **17**/**4**, 599 (1998).
16. Conradson, S. D.: Appl. Spectrosc. **52**, 252 (1998).
17. Reich, T., Geipel, G., Hennig, C., Roßberg, A., Bernhard, G.: First EXAFS Measurement of Plutonium Solutions at ROBL. Institut für Radiochemie, Forschungszentrum Rossendorf, Annual Report (1999) p. 72.
18. Knopp, R., Panak, P. J., Wray, L. A., Renninger, N., Keasling, J. D., Nitsche, H.: Laser spectroscopic studies of interactions of U(VI) with bacterial phosphate species. Submitted.
19. Panak, P. J., Knopp, R., Booth, C. H., Nitsche, H.: Spectroscopic studies on the interaction of U(VI) with *Bacillus sphaericus*. Submitted.
20. Lawrence, J. M., Riseborough, P. S., Booth, C. H., Sarro, J. L., Thompson, J. D. Osborn, R.: Phys. Rev. B **63**, 054427 (2001).